The Journal of Chemical Physics

Theory of vibrational polariton chemistry in the collective coupling regime

Cite as: J. Chem. Phys. **156**, 014101 (2022); https://doi.org/10.1063/5.0074106
Submitted: 06 October 2021 • Accepted: 12 December 2021 • Accepted Manuscript Online: 13 December 2021 • Published Online: 03 January 2022

Arkajit Mandal, Xinyang Li and Pengfei Huo

The Journal of Chemical Physics ARTICLE scitation.org/journal/jcp

Theory of vibrational polariton chemistry in the collective coupling regime

Cite as: J. Chem. Phys. 156, 014101 (2022); doi: 10.1063/5.0074106
Submitted: 6 October 2021 • Accepted: 12 December 2021 •
Published Online: 3 January 2022

Arkajit Mandal,[1,a] Xinyang Li,[1] and Pengfei Huo[1,2,b]

AFFILIATIONS

[1] Department of Chemistry, University of Rochester, Rochester, New York 14627, USA
[2] Hajim School of Engineering and Applied Sciences, Institute of Optics, University of Rochester, Rochester, New York 14627, USA

Note: This paper is part of the 2021 JCP Emerging Investigators Special Collection.
[a] **Electronic mail:** amandal4@ur.rochester.edu
[b] **Author to whom correspondence should be addressed:** pengfei.huo@rochester.edu

ABSTRACT

We theoretically demonstrate that the chemical reaction rate constant can be significantly suppressed by coupling molecular vibrations with an optical cavity, exhibiting both the collective coupling effect and the cavity frequency modification of the rate constant. When a reaction coordinate is strongly coupled to the solvent molecules, the reaction rate constant is reduced due to the dynamical caging effect. We demonstrate that collectively coupling the solvent to the cavity can further enhance this dynamical caging effect, leading to additional suppression of the chemical kinetics. This effect is further amplified when cavity loss is considered.

I. INTRODUCTION

Inside an optical cavity, hybridizing molecular vibrations and photonic excitations[1–3] form vibrational polaritons [Fig. 1(a)]. Several recent experiments[3–9] have demonstrated that it is possible to modify ground-state chemical reactions by coupling the cavity radiation mode with the vibrational degrees of freedom (DOF) of molecules. This new strategy of vibrational strong coupling (VSC), if feasible, will offer a paradigm shift in chemical transformations.[3,5]

Despite recent theoretical progress,[10–18] a clear theoretical explanation of such remarkable VSC effects in ground-state reactivity remains elusive, including explanations of both (i) the collective effect ($\sqrt{N}$-dependent effect, where N is the total number of molecules inside the cavity) on chemical reaction rates, and (ii) the resonant effect, where the suppression of the rate is achieved with a particular cavity photon frequency.

Our previous work[12] suggests that the VSC modification of the rate constant is purely dynamical, originating from the caging effect of the cavity mode coupled to the reaction coordinate, as opposed to modifying the reaction barrier height.[15,19] However, these previous theoretical discussions are often limited to the case of a single molecule[12,16] or a few molecules[20] coupled to the cavity. It is thus an open question whether these theoretical explanations also survive to the large N limit and exhibit the collective effect.[17,19,21] On the other hand, both effects do show up in a VSC non-adiabatic electron transfer reaction[11,22] with an enhancement of the rate upon resonant coupling between molecular vibration and the cavity, although the applicability of this theory on the VSC ground-state adiabatic reactions remains an open question. Similarly, in the recent theoretical work of vibrational energy transfer, one can exhibit both the resonant effect and the collective effect for these energy transfer rates.[10] However, their connection to the chemical reaction rate constant remains to be discussed. Finally, recent theoretical works[17,23] have suggested a coherent mechanism where collective coupling effects appear if "the polariton is activated collectively to the transition state"[17] such that the chemical reaction occurs via the collective bright mode comprising all reaction coordinates. However, the physical origin of such a collective mechanism remains unclear.[15]

In this work, we theoretically demonstrate that the chemical reaction rate constant can be modified when a set of solvent DOF is collectively coupled to both a reaction coordinate of a solute molecule and the cavity radiation mode. Our results demonstrate both the collective coupling effect and the cavity frequency-dependent modifications of the reaction rate constant,[3,5] which

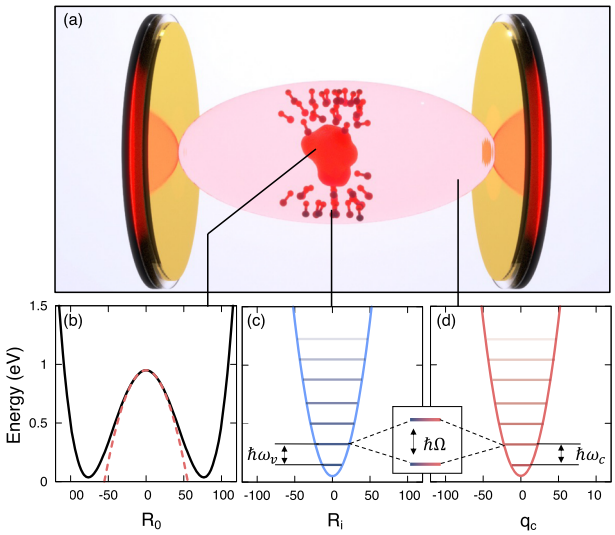

FIG. 1. (a) Schematic illustration of the reactive molecule coupled to a set of solvent modes (phonon), which are, in turn, coupled to the quantized radiation mode in a cavity. (b) Double-well potential (black solid line) for a chemical reaction as a function of the reaction coordinate R_0 where the barrier can be approximated as an inverted Harmonic potential (red dashed line). (c) Potential energy of a harmonic phonon mode (solvent) and (d) a bare cavity mode. The vibrational state and photon state hybridization leads to a Rabi splitting $\hbar\Omega_R$.

purely originate from a change of the transmission coefficient (recrossing factor) of the rate constant due to the dynamical caging effects from the cavity.[12]

II. THEORY AND THE MODEL SYSTEM

We begin by writing the light–matter interaction Hamiltonian in the minimal coupling form as follows:

$$\hat{H}_{\rm C} = \sum_j \frac{1}{2m_j}\left(\hat{\mathbf{p}}_j - z_j\hat{\mathbf{A}}\right)^2 + \hat{V}(\hat{\mathbf{x}}) + \hat{H}_{\rm ph}, \tag{1}$$

where the sum is performed over all charged particles, including both electrons and nuclei; m_j and z_j are the mass and charge for particle j, respectively; and $\hat{V}$ represents the Coulomb potential of all charged particles. The total dipole operator of the matter is $\hat{\boldsymbol{\mu}} = \sum_j z_j x_j$. In addition, $\hat{\mathbf{x}} \equiv \{\hat{\mathbf{x}}_j\} = \{\hat{\mathbf{R}}, \hat{\mathbf{r}}\}$ with $\hat{\mathbf{R}}$ and $\hat{\mathbf{r}}$ representing the nuclear and electronic coordinates, respectively, $\hat{\mathbf{p}} \equiv \{\hat{\mathbf{p}}_{\mathbf{R}}, \hat{\mathbf{p}}_{\mathbf{r}}\} \equiv \{\hat{\mathbf{p}}_j\}$ is the canonical momentum operator such that $\hat{\mathbf{p}}_j = -i\hbar\nabla_j$. The cavity photon field Hamiltonian under the single mode assumption is expressed as $\hat{H}_{\rm ph} = \hbar\omega_{\rm c}\left(\hat{a}^\dagger\hat{a} + \frac{1}{2}\right) = \frac{1}{2}\left(\hat{p}_{\rm c}^2 + \omega_{\rm c}^2\hat{q}_{\rm c}^2\right)$, where $\omega_{\rm c}$ is the frequency of the mode in the cavity, $\hat{a}^\dagger$ and $\hat{a}$ are the photonic creation and annihilation operators, and $\hat{q}_{\rm c} = \sqrt{\hbar/2\omega_{\rm c}}(\hat{a}^\dagger + \hat{a})$ and $\hat{p}_{\rm c} = i\sqrt{\hbar\omega_{\rm c}/2}(\hat{a}^\dagger - \hat{a})$ are the photonic coordinate and momentum operators, respectively. Choosing the Coulomb gauge, $\nabla\cdot\hat{\mathbf{A}} = 0$, the vector potential becomes purely transverse as $\hat{\mathbf{A}} = \hat{\mathbf{A}}_\perp$. Under the long-wavelength approximation, $\hat{\mathbf{A}} = \mathbf{A}_0\left(\hat{a} + \hat{a}^\dagger\right) = \mathbf{A}_0\sqrt{2\omega_{\rm c}/\hbar}\ \hat{q}_{\rm c}$ for a Fabry–Pérot cavity, where $\mathbf{A}_0 = \sqrt{\hbar/2\omega_{\rm c}\varepsilon_0\mathcal{V}}\cdot\hat{\mathbf{e}}$, with $\mathcal{V}$ as the quantization volume inside the cavity, ε_0 as the permittivity, and $\hat{\mathbf{e}}$ as the unit vector of field polarization.

Using the Power–Zienau–Woolley (PZW)[24,25] gauge transformation operator $\hat{U} = \exp\left[-\frac{i}{\hbar}\hat{\boldsymbol{\mu}}\cdot\mathbf{A}_0\left(\hat{a} + \hat{a}^\dagger\right)\right]$ and the unitary phase transformation operator $\hat{U}_\phi = \exp[-i\frac{\pi}{2}\hat{a}^\dagger\hat{a}]$, the Pauli–Fierz (PF) non-relativistic QED Hamiltonian[26,27] $\hat{H}_{\rm PF} = \hat{U}_\phi\hat{U}\hat{H}_{\rm C}\hat{U}^\dagger\hat{U}_\phi^\dagger$ is obtained as follows:

$$\hat{H}_{\rm PF} = \hat{H}_m + \frac{1}{2}\hat{p}_{\rm c}^2 + \frac{1}{2}\omega_{\rm c}^2\left(\hat{q}_{\rm c} + \sqrt{\frac{2}{\hbar\omega_{\rm c}}}\hat{\boldsymbol{\mu}}\cdot\mathbf{A}_0\right)^2, \tag{2}$$

where the matter Hamiltonian is $\hat{H}_m = \hat{T}_{\mathbf{R}} + \hat{T}_{\mathbf{r}} + \hat{V}$, with $\hat{T}_{\mathbf{R}}$ and $\hat{T}_{\mathbf{r}}$ representing the nuclear and electronic kinetic energies, respectively. The presence of the dipole self-energy (DSE) term $\frac{\omega_{\rm c}}{\hbar}\left(\hat{\boldsymbol{\mu}}\cdot\mathbf{A}_0\right)^2$ in Eq. (2) is necessary in order to have a gauge invariant Hamiltonian,[26–28] and it has shown to be crucial for an accurate description of light–matter interactions under the dipole gauge.[26,27,29]

In Sec. I of the supplementary material, we started the theoretical derivation for the most general case of the molecular dipole orientation with respect to the field polarization direction. We found that when the molecules have an isotropic distributions, there is no collective VSC modification on the reaction rate constant (see Sec. I B in the supplementary material). This also agrees with the other recent theoretical findings.[19] We, thus, assume that the dipole of the matter is oriented in the field polarization direction such that $\hat{\boldsymbol{\mu}}\cdot\mathbf{A}_0 = \hat{\mu}\cdot A_0$, and this should be viewed as an additional assumption. We should note that in the VSC experiments,[3,5] the molecules are more likely to have a completely isotropic distribution with respect to the cavity polarization direction. On the other hand, it is certainly possible to have chemical reactions in anisotropic solvents, such as liquid crystals[30–32] inside an optical cavity.[33]

Because all these VSC experiments[3–8] are performed with electronically adiabatic reactions in the ground adiabatic states, we only consider the electronic ground state of the system defined as

$$\left(\hat{H}_m - \hat{T}_{\mathbf{R}}\right)|\Psi_g(\mathbf{R})\rangle = E_g(\mathbf{R})|\Psi_g(\mathbf{R})\rangle, \tag{3}$$

where $E_g(\mathbf{R})$ is the ground adiabatic potential and $|\Psi_g(\mathbf{R})\rangle$ is the ground adiabatic electronic state of the matter. Projecting $\hat{H}_m$ and $\hat{\mu}$ in the ground electronic state with $\hat{\mathcal{P}} = |\Psi_g\rangle\langle\Psi_g|$, we obtain the following model Hamiltonian:

$$\hat{\mathcal{H}}_{\rm PF}^g = \frac{\hat{\mathbf{p}}^2}{2} + E_g(\mathbf{R}) + \frac{\hat{p}_{\rm c}^2}{2} + \frac{1}{2}\omega_{\rm c}^2\left(\hat{q}_{\rm c} + \sqrt{\frac{2}{\hbar\omega_{\rm c}}}A_0\cdot\mu_g(\mathbf{R})\right)^2, \tag{4}$$

where $\mu_g(\mathbf{R}) = \langle\Psi_g|\hat{\mu}|\Psi_g\rangle$. Note that projecting $\hat{\mu}$ inside the dipole self-energy term is the accurate matter state truncation scheme for the dipole-gauge Hamiltonian[28,29] because it ensures that all operators are properly confined in the same truncated electronic subspace $\hat{\mathcal{P}} = |\Psi_g\rangle\langle\Psi_g|$ in order to generate consistent results compared to the full Hamiltonian.[34]

In this work, we consider a model system for $E_g(\mathbf{R})$, where $\mathbf{R} = \{R_0, R_1, \ldots, R_N\}$ include a reactive molecule with a single reaction coordinate R_0 and N solvent DOFs R_i (where $i \in [1, N]$) that

couples to R_0. Using the typical Caldeira–Leggett[35] system–bath Hamiltonian, $E_g(\mathbf{R})$ is modeled as

$$E_g(\mathbf{R}) = U_0(R_0) + \sum_{i=1}^{N} \frac{1}{2}\omega_i^2 \left(R_i + \frac{c_i}{\omega_i^2} R_0 \right)^2. \quad (5)$$

The solute molecule is modeled as a double-well potential $U_0(R_0) = a \cdot R_0^4 - b \cdot R_0^2$, as shown in Fig. 1(b) (solid black line), to represent the chemical reaction along R_0, and the details of the parameters are provided in Sec. V of the supplementary material. At the top of the barrier $R_0 = R_0^{\ddagger}$, $U_0(R_0) \approx -\frac{1}{2}\omega_{\ddagger}^2 (R_0 - R_0^{\ddagger})^2$ as indicated by the red dashed line in Fig. 1(b), where $\omega_{\ddagger} = 1048\ \mathrm{cm}^{-1}$ is the top of the barrier frequency. Furthermore, the total dipole of the system is $\mu_g(\mathbf{R}) = \sum_{i=1}^{N} \mu_i(R_i)$, and we assume that $\mu_0(R_0) = 0$. Note that the coupling strength between the cavity mode and individual molecules is very weak under the collective coupling regime; thus, the result of this work does not change if $\mu_0(R_0) \neq 0$. We further simplify our consideration of the solute–solvent coupling as $c_i = c_s$ and $\omega_i = \omega_s = 1400\ \mathrm{cm}^{-1}$, where we denote ω_s as the solvent vibrational frequency for all modes $i \in [1, N]$. These values are typical for nuclear vibrations and are within the range of the recent experiments of VSC modified reactivities,[3,4] ranging from 800 to 3000 cm^{-1}. The amplitude of the solvent friction is $\lambda = \sum_{i=1}^{N} \frac{c_i^2}{\omega_i^2} = N c_s^2/\omega_s^2$. In this work, we keep λ as a constant throughout. This means that as we increase N, the corresponding c_s will be decreased by $1/\sqrt{N}$ and the overall solvent–solute interactions characterized by λ will not change as we increase N. In particular, we use $\lambda = 3.84 \times 10^{-4}$ a.u., and for $N = 2500$, which corresponds to the solvent–solute coupling as $c_s = 2.5 \times 10^{-6}$ a.u. The physical solvent–solute interactions require a distribution of values for c_i that satisfies a particular spectral density. Further generalization of the solvent–solute coupling c_i with an arbitrary spectral density is possible,[36] with the details provided in Sec. I C of the supplementary material. On the other hand, the light–matter coupling strength A_0 in Eq. (4) is kept fixed, corresponding to the situation where the cavity-per-molecule coupling is a constant. Thus, the collective coupling between the molecules and the cavity[2,5] increases as one increases N, which shows up in both the Rabi splitting and modification of the reaction rate constant.

The physical realization of our model reaction in Eq. (5) could be the proton transfer reaction in the ground state, where the proton transfer coordinate R_0 couples to many solvent molecules due to the long-range electrostatic interactions.[37–41] A well-established model of this problem is the Azzouz–Borgis model[42–47] in theoretical literature, where the proton transfer coordinate often effectively couples to more than hundreds of explicit solvent molecules. One can also extract the global solvent coordinate that couples to the reaction coordinate.[48–50] The cavity mode, on the other hand, interacts with all solvent modes, resulting in delocalized interactions that can be observed from the Rabi splitting from spectroscopy.[2] For the solvent–solute interactions, with an increase in the number of solvent molecules, the outer sphere solvents will only be weakly coupled to the solute, while the inner sphere solvent strongly coupled to the solute, resulting in a solute–solvent distance specific coupling strength c_i. Here, we consider a simplified picture in which we scale all c_i values to be smaller when we increase N such that λ is fixed. In Sec. I C of the supplementary material, we have considered the case of distributions of c_i and we found that the collective effects survive. On the other hand, our model reaction in Eq. (5) cannot describe reactions that involve local covalent bond-breaking, where the reaction coordinate is likely only locally coupled to a few solvent molecules in the immediate neighborhood of the solute.

Treating both $\mathbf{R}$ and q_c in Eq. (4) on an equally classical footing,[10,12,15,19,21] the VSC polariton chemical kinetics can be viewed as a barrier crossing process on the cavity Born–Oppenheimer surface (CBO),[51]

$$E_{\mathrm{CBO}}(\mathbf{R}, q_c) = E_g(\mathbf{R}) + \frac{1}{2}\omega_c^2 \left(\hat{q}_c + \sqrt{\frac{2}{\hbar\omega_c}} A_0 \cdot \mu_g(\mathbf{R}) \right)^2. \quad (6)$$

One can then express the reaction rate constant as follows:[52–54]

$$k = \lim_{t \to t_p} \kappa(t) \cdot k_{\mathrm{TST}}, \quad (7)$$

where k_{TST} is the Transition State Theory (TST) rate constant and t_p is the plateau time of the transmission coefficient $\kappa(t)$. It has been shown that the classical potential of mean force (free energy profile) is invariant under the change of light–matter coupling strength or the photon frequency.[15] Other theoretical investigations based on a simple TST analysis also suggest no significant change of the reaction rate constant.[19,55] The TST rate[56] is expressed as $k_{\mathrm{TST}} = \frac{\omega_0}{2\pi} e^{-\beta E^{\ddagger}}$, where $E^{\ddagger} = E_{\mathrm{CBO}}(R_0^{\ddagger}) - E_{\mathrm{CBO}}(R_0^{\mathrm{eq}})$ is the CBO potential energy barrier height measured from the bottom of the well R_0^{eq} to the top of the barrier $R_0^{\ddagger}$, $\omega_0 \approx 1484\ \mathrm{cm}^{-1}$ is the vibrational frequency of the reactant at $R = R_0^{\mathrm{eq}}$ on the E_{CBO} [Eq. (6)], and $\beta = (k_B T)^{-1}$. When the DSE is explicitly considered, $E^{\ddagger}$ remains invariant to changes of the light–matter coupling strength or the photon frequency. This is because the equilibrium position along the photonic coordinate q_c is $q_c^0(\mathbf{R}) = -\sqrt{\frac{2}{\hbar\omega_c}} A_0 \cdot \mu_g(\mathbf{R})$ for all possible $\mathbf{R}$ (for more details, see Sec. II of the supplementary material). Thus, the last term in Eq. (6) is always 0 for the stationary points (either a minimum or a transition state) on the cavity BO surface. This explains why one cannot observe any effects from a simple TST analysis when treating q_c classically.[15,19,55] A recent work[57] on VSC chemistry treating q_c quantum mechanically suggests that even when the zero-point energy along q_c is fully considered, the change of $E^{\ddagger}$ is less than 20 cm^{-1} across a large range of coupling strengths.

The transmission coefficient captures the dynamical recrossing effects through the flux-side correlation function formalism,[52–54]

$$\kappa(t) = \frac{\left\langle \mathcal{F}(0) \cdot h\left[R_0(t) - R_0^{\ddagger}\right] \right\rangle}{\left\langle \mathcal{F}(0) \cdot h\left[\dot{R}_0^{\ddagger}(0)\right] \right\rangle}, \quad (8)$$

where $h[R_0 - R_0^{\ddagger}]$ is the Heaviside function of the reaction coordinate R_0 with the dividing surface $R_0^{\ddagger}$ that separates the reactant and the product regions (for the model system studied here, $R_0^{\ddagger} = 0$), the flux function $\mathcal{F}(t) = \dot{h}(t) = \delta[R_0(t) - R_0^{\ddagger}] \cdot \dot{R}_0(t)$ measures the reactive flux across the dividing surface [with $\delta(R)$ as the Dirac delta function], $\dot{R}_{\ddagger}(0)$ represents the initial velocity of the nuclei on the dividing surface, and $\langle \cdots \rangle$ represents the canonical ensemble average with the constraint on the dividing surface enforced by $\delta[R(t) - R_0^{\ddagger}]$ inside $\mathcal{F}(t)$. Since k_{TST} does not change under the

VSC condition, we have conjectured[12] that VSC chemical reactivities purely originate from the transmission coefficient κ. Based on this, we have demonstrated the cavity frequency dependence of the VSC modification of κ for a single molecule coupled to the cavity.[12] In this work, we consider the scenario in which such a cavity modification can also be observed in the collective coupling regime.

We numerically compute $\kappa(t)$ using the flux-side correlation function formalism in Eq. (8) with the details provided in Sec. V of the supplementary material. On the other hand, $\kappa = \lim_{t\to t_p}\kappa(t)$ can also be obtained using the Grote–Hynes (GH) theory[56,58–62] through the multidimensional transition-state treatment.[56,63–65] The transmission coefficient using the GH theory is

$$\kappa_{\rm GH} = \frac{1}{\omega_\ddagger}\sqrt{-(\Omega_-^\ddagger)^2}, \tag{9}$$

where $\Omega_-^\ddagger$ is the unstable imaginary normal-mode frequency at the dividing surface $R_0 = R_0^\ddagger$. To obtain $\Omega_-^\ddagger$, we further approximate the dipole of the ith solvent molecule around its equilibrium position $R_i = 0$ as $\mu_i(R_i) \approx \mu_0 + \mu' R_i$, where $\mu_0 = \mu(R_i = 0)$ and $\mu' = \frac{\partial \mu_g(R_i)}{\partial R_i}|_{R_i=0}$, and define the collective bright mode of the solvent[19] as $R_{\rm B} = \frac{1}{\sqrt{N}}\sum_{i=1}^N R_i$. The QED Hamiltonian $\mathcal{H}_{\rm PF}^g$ can be shown to have three coupled modes, $\mathbf{x} = \{R_0, R_{\rm B}, q_c\}$, whereas the rest of the normal modes (commonly referred to as the dark modes[19]) are completely decoupled. At the dividing surface $R_0 = R_0^\ddagger$, the Hessian matrix in the three-mode $\mathbf{x}$ subspace is

$$\mathcal{H}_{\mathbf{x}} \equiv \frac{\partial^2 \mathcal{H}_{\rm PF}^g}{\partial x_i \partial x_j} = \begin{bmatrix} -\omega_\ddagger^2 + N\frac{c_{\rm s}^2}{\omega_{\rm s}^2} & \sqrt{N}c_{\rm s} & 0 \\ \sqrt{N}c_{\rm s} & \omega_{\rm s}^2 + N\frac{\mathcal{C}^2}{\omega_c^2} & \sqrt{N}\mathcal{C} \\ 0 & \sqrt{N}\mathcal{C} & \omega_{\rm c}^2 \end{bmatrix}, \tag{10}$$

where $\mathcal{C} = A_0\mu'\sqrt{\frac{2\omega_{\rm c}^3}{\hbar}}$ and N is the number of solvent DOFs. A detailed derivation of Eq. (10) is provided in Sec. I A of the supplementary material. The imaginary frequency $\Omega_-^\ddagger$ can be obtained by diagonalizing $\mathcal{H}_{\mathbf{x}}$ in Eq. (10). The key to the emerging collective VSC effects is the $\sqrt{N}c_s$ term and $\sqrt{N}\mathcal{C}$ in the above Hessian matrix, which does not exist if one ignores dipole self-energies or considers N solute molecules (with potential U_0) coupled to the cavity.[19]

While $\Omega_-^\ddagger$ can be easily computed by numerically diagonalizing Eq. (10), a simple and concise analytical expression for $\Omega_-^\ddagger$ is not readily available. Nonetheless, we find an approximate expression of $\Omega_-^\ddagger$ (see the detailed derivation in Sec. III of the supplementary material) as follows:

$$\Omega_-^\ddagger \approx \left[\frac{1}{2}\left(\tilde{\omega}_\ddagger^2 - \omega_{\rm c}^2\right) + \frac{1}{2}\sqrt{\left(\omega_{\rm c}^2 + \tilde{\omega}_\ddagger^2\right)^2 + 4N\sin^2\Theta_\ddagger \mathcal{C}^2}\right]^{1/2}, \tag{11}$$

where $-\tilde{\omega}_\ddagger^2 = \frac{1}{2}\left(-\omega_\ddagger^2 + N\frac{c_{\rm s}^2}{\omega_{\rm s}^2} + \omega_{\rm s}^2 + N\frac{\mathcal{C}^2}{\omega_{\rm c}^2}\right) - \frac{1}{2}\sqrt{\left(\omega_\ddagger^2 - N\frac{c_{\rm s}^2}{\omega_{\rm s}^2} + \omega_{\rm s}^2 + N\frac{\mathcal{C}^2}{\omega_{\rm c}^2}\right)^2 + 4Nc_{\rm s}^2}$ and $\Theta_\ddagger = \frac{1}{2}\tan^{-1}\left[2\sqrt{N}c_{\rm s}/\left(-\omega_\ddagger^2 + N\frac{c_{\rm s}^2}{\omega_{\rm s}^2} - \omega_{\rm s}^2 - N\frac{\mathcal{C}^2}{\omega_{\rm c}^2}\right)\right]$. It is interesting to note that Eq. (11) has a similar (but not identical) structure as the case of a single molecule coupled to the cavity.[12] That said, the dependence of $\Omega_-^\ddagger$ (or $\kappa_{\rm GH}$) on ω_c is complicated as both $\Theta_\ddagger$ and $\tilde{\omega}_\ddagger$ depend on ω_c in a non-trivial fashion. Nevertheless, one can clearly see from Eqs. (10) and (11) that $\Omega_-^\ddagger$ depends on both $\omega_{\rm c}$ and N, giving rise to the cavity frequency dependence and the collective coupling effect. Furthermore, both $\Omega_-^\ddagger$ and $\kappa_{\rm GH}$ are functions of $\sqrt{N}\mu'$, which is a signature of the collective coupling effect. This is similar to the collective Rabi splitting $\hbar\Omega$, which depends on $\sqrt{N}\mu'$ when hybridizing the solvent modes $\{R_i\}$ to the cavity mode $q_{\rm c}$ [as shown in Figs. 1(c) and 1(d)].

In the Travis–Cummings model, under the resonant condition when $\omega_{\rm s} = \omega_{\rm c}$, $\hbar\Omega$ is given as

$$\hbar\Omega = \sqrt{N}\mu' A_0\sqrt{2\hbar\omega_{\rm s}} \equiv 2\eta\cdot\hbar\omega_{\rm c}, \tag{12}$$

where the unitless parameter η (defined above) characterizes the normalized light–matter coupling strength. On the other hand, the transmission coefficient based on Eq. (11) is minimized at a different frequency, which we denote as $\omega_{\rm c}^0$. This frequency has a dependence of both *omega*$_{\rm s}$ and $\omega_\ddagger$, as later shown in our numerical results.

III. RESULTS AND DISCUSSION

Figure 2 demonstrates both (a) the cavity frequency dependence and (b) the collective effects on modifying the reaction rate constant. Outside the cavity, the transmission coefficient in the absence of light–matter interaction is $\kappa(\eta = 0) = \kappa_0 \approx 0.317$, which is much lower than 1 due to solvent molecules coupled to the reaction coordinate R_0 around the barrier region. This choice is within the range of many chemical reactions, for example, $\kappa_0 \approx 0.3$–0.5 in Refs. 66 and 67. Since $k_{\rm TST}$ remains invariant for all results presented in this work, we only use the change of κ to characterize the VSC modification of the reactivities.

Figure 2(a) presents the results of coupling $N = 2500$ solvent DOFs to the cavity and obtaining κ using both the GH theory (solid lines) and the direct numerical simulations (dotted lines) using Eq. (8). The results from both approaches are nearly identical. Importantly, we observe a strong dependence of κ on the photon frequency $\hbar\omega_{\rm c}$, and κ is minimized at a certain photon frequency, which we refer to as $\omega_{\rm c}^0$. While we do not have a simple analytic expression

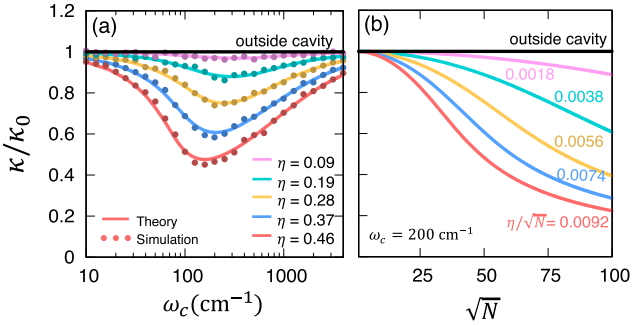

FIG. 2. (a) Cavity frequency-dependent suppression of the transmission coefficient κ (where κ_0 represents the cavity-free scenario) as a function of the cavity photon frequency $\omega_{\rm c}$ with $N = 2500$ solvent modes at various collective light–matter coupling strengths η. (b) κ as a function of N while keeping collective solvent–solute coupling $\sqrt{N}c_{\rm s}$ a constant.

of ω_c^0 (which can be, in principle, obtained from $\partial\kappa_{GH}/\partial\omega_c = 0$), it is a function of ω_s, $\omega_\ddagger$, c_s, and η [see its definition in Eq. (12)]. As shown, an increase in η results in a significant redshift in ω_c^0, which has not been observed experimentally. Interestingly, this redshift is also observed in a recent quantum TST theory, assuming a coherent polariton activation mechanism [see Fig. 4(b) in Ref. 17]. This is likely due to the fact that we (see Ref. 17) assume a perfect cavity, whereas in the real VSC experiments,[3,5] the optical cavity often has a very low-quality factor. When explicitly including the cavity loss (as shown in Fig. 3), ω_c^0 also shifted back to the value closer to ω_c.

Note that η signifies collective coupling, and the individual solvent–cavity coupling is weak ($\eta/\sqrt{N} < 0.0093$). However, we should point out that the coupling strength is still larger than the estimated values in the experiments (which typically have $N \approx 10^9$–10^{10} molecules effectively coupled to the cavity) with a normalized coupling *eta* [see definition in Eq. (12)] ranging from $\eta = 0.03$–0.06[3,5] to $\eta = 0.1$.[6] Nevertheless, our model calculations clearly demonstrate the same essential feature of the collective coupling effects observed in the experiments, which is the rate constant suppression as increasing the number of molecules (or the concentration of the molecules).[5]

We emphasize that the suppression of the κ is originated from the collective dynamical caging effects, where the cavity radiation mode is effectively acting as an additional "solvent" DOF coupled to the collective bright solvent coordinate R_B, which, in turn, coupled to the reactive coordinate R_0 such that the presence of the cavity mode enhances the recrossing of the reaction coordinate and reduces the transmission coefficient. As a result, with an increase in light–matter coupling strength, the plateau value of $\kappa(t)$ keeps decreasing and, at the same time, becomes more oscillatory [see Fig. S3 of the supplementary material (Sec. V)]. This phenomenon is well explored in the context of solvent-mediated dynamical caging effects.[56,59,68–70] More detailed discussions on the dynamical caging hypothesis of the VSC reaction can be found in Ref. 12. We should point out that the resonance condition for the modification of the reaction rate in Fig. 2(a) is much wider than the narrower resonant condition observed in the experiments.[4] We suspect that this is due to the purely classical treatment of q_c, and a quantum mechanical treatment of q_c should give a narrower resonant condition. This has been recently discussed in a quantum TST-based theoretical analysis.[17]

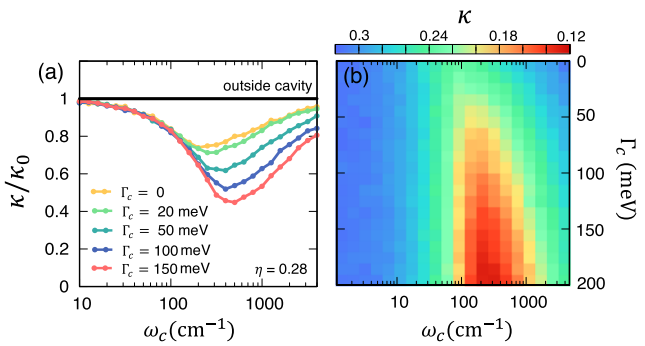

FIG. 3. Transmission coefficient κ when explicitly considering the cavity loss Γ_c at $\eta = 0.28$. (a) Cavity frequency dependence of the transmission coefficient κ at various Γ_c. (b) κ as a function of photon frequency and cavity loss Γ_c.

Figure 2(b) demonstrates the N-dependence of the transmission coefficient using the GH theory while keeping ω_c constant. Note that to clearly identify the effect of increasing N on the light–matter interactions, we have kept λ a constant. We find that the increase in N effectively increases the light–matter interaction strength [see Eq. (12)], leading to an additional suppression of chemical kinetics. Interestingly, unlike the $\hbar\Omega$, which linearly depends on $\sqrt{N}$ [see Eq. (12)], κ has a non-linear monotonic dependence of $\sqrt{N}$. This theoretical prediction agrees with the recent VSC experiments by Ebbesen and co-workers [such as Fig. 3(d) in Ref. 5 and Fig. 3(a) in Ref. 4].

Up until now, we have considered a perfect microcavity setup with no photon leaking. Despite the recent progress in the development of high-quality factor Fabry–Pérot cavities, optical microcavities are generally leaky. The typical values of cavity losses for a Fabry–Pérot cavity is in the range of $\Gamma_c = 5$–100 meV.[3,71–73] In the classical Markovian limit, the cavity loss (dissipation) can be described with Langevin dynamics of the cavity radiation mode (see Sec. III of the supplementary material for derivations), with the equation of motion

$$\ddot{q}_c = -\frac{d\mathcal{H}_{PF}^g}{dq_c} - \Gamma_c p_c + F_c(t), \tag{13}$$

where Γ_c is the cavity loss rate and $F_c(t)$ is a Gaussian random force bounded by the fluctuation–dissipation theorem through $\langle F_c(0)F_c(t)\rangle = 2\Gamma_c k_B T\delta(t)$. Using this approach, we can numerically compute κ using the flux-side correlation function expression in Eq. (8). Incorporating such dissipative dynamics in the GH theory makes it nontrivial to derive a simple analytic expression for κ_{GH}, and therefore, we study the effect of the cavity loss only through direct numerical simulations.

Figure 3 demonstrates the effect of cavity loss on κ. Here, we choose $\eta = 0.28$ and keep $N = 2500$ (with per-molecule coupling $\eta/\sqrt{N} = 0.0056$) as a constant while varying the cavity loss rate Γ_c. In Fig. 3(a), we observe that increasing Γ_c results in further suppression of the chemical rate constant while concurrently blueshifting the maximum suppression frequency ω_c^0. It can be seen in Fig. 3(b) that an increase in Γ_c shifts ω_c^0 gradually toward the value of ω_0, which is the vibrational frequency of the solvent molecules. This cavity loss-assisted suppression of chemical kinetics can be attributed to the fact that the cavity loss dynamics arises when the cavity mode is coupled to other non-cavity radiation modes, which act as additional dissipative baths[74] (see Sec. IV of the supplementary material). Just like the cavity mode which acts like a dissipative bath to the collective solvent coordinate R_B that leads to suppression of chemical kinetics (as shown in Fig. 2), introducing an additional dissipative environment to the cavity mode itself also leads to further suppression of the chemical rate constant. Note that when explicitly considering cavity loss dynamics, the collective coupling effects (Fig. 2) still persist, as demonstrated in Sec. IV of the supplementary material.

IV. CONCLUSIONS AND FUTURE PERSPECTIVES

In conclusion, we theoretically demonstrate both the collective coupling effects and the cavity frequency-dependent modifications

of the reaction rate constant in the polaritonic vibrational strong coupling regime. The suppression in chemical kinetics is cavity photon-frequency-dependent such that maximal suppression occurs around a particular photon frequency ω_c^0. Outside the cavity, when a collective solvent mode is strongly coupled to a reaction coordinate in the non-Markovian limit, the reaction coordinate becomes dynamically caged near the barrier region. When coupling to the cavity, we find that the cavity radiation mode and intrinsic cavity loss assist in dynamical caging of the reaction coordinate, leading to further suppression of the reaction rate constant if the solvent dipoles are aligned in the cavity polarization direction. This effect operates under the collective coupling regime and survives when per-molecule (per-solvent DOF) light–matter coupling is weak.

We should emphasize that by no means, this theoretical work provides the ultimate answer to the mysteries of the VSC modification of the reactivities. Future work should aim to address the following limitations of this work.

(1) The resonant condition. Experimentally, the resonant condition is referred to as when the cavity frequency ω_c matches the frequency of the vibration ω_s such that it generates a large vibrational polariton Rabi splitting under the condition $\omega_c = \omega_s$ [see Eq. (12)]. It is also believed that[3,4] the maximum reduction of the rate constant is achieved by tuning the cavity frequency ω_c^0 to match the same bond vibrational frequency ω_s. Our theoretical work, on the other hand, predicts that a maximum reduction of the rate constant (purely through transmission coefficient) is achieved by matching ω_c^0 to a value determined by both the top of the barrier frequency of the reaction coordinate $\omega_\ddagger$ and the equilibrium vibrational frequency ω_s [see Eq. (11)]. Note that in a recent work based on quantum TST, the maximum reduction of the rate constant is related to both the vibrational frequency (through the quantum entropy correction) and the reactive barrier frequency (through κ_{GH}, as we have shown in our previous work[12]) is high. Thus, it might suggest that our current results (as well as those in Ref. 17) are inconsistent with the experimental results. Interestingly, a significant rate suppression can also be achieved without perfectly matching the cavity frequency with any bond vibrational frequency ω_s; for example, see Fig. 3A in Ref. 3 for the rate constant reduction peak around 1250 cm^{-1}. Thus, a precise experimental measurement on the value of ω_c^0 and its relation with ω_s will be extremely valuable to further scrutinize different theories.

(2) Disorders of molecular orientations. Our current theory requires all solvent molecules to be perfectly aligned with the quantized radiation mode inside the cavity. The VSC experiments take place in the solution, where the molecules should, in principle, be isotropically distributed. Future theoretical work needs to focus on releasing the requirement of perfect alignment of all solvent molecules and allowing isotropic disorder of the molecules. On the other hand, the current experiments[33] can already achieve strong light–matter couplings between anisotropic solvents, such as liquid crystals[30,31] inside an optical cavity.[32,33] Thus, it will be interesting to test this theoretical prediction in its current form for chemical reactions within those liquid crystals inside an optical cavity.

(3) Enhancement of the rate constant. There are also VSC experiments suggesting that the rate constants can be enhanced[8,75] by a large amount when solvent DOFs are coupled to the cavity, although the validity of the observed enhancement for some experiments[76] is still subject to debate.[76,77] This theoretical framework cannot explain such a significant enhancement of the rate constant due to coupling to the cavity. Classically, the Kramers turnover theory predicts that in the under-damped regime, an increase in the system–bath friction will first enhance the rate constant, then approach the plateau regime of the rate constant, and finally reach the over-damped regime that decreases the rate constants. Coupling the cavity mode (photonic environment) could enhance the reaction rate constant if the reaction is originally in the under-damped regime. However, it is hard to believe that the reactions investigated in those experiments are in that regime,[8] and future theoretical work is required to fully understand this behavior.

We envision that this theoretical work brings us one step closer to finally resolving the mysteries of VSC enabled chemistry demonstrated in recent experiments[3–8] by demonstrating both the collective coupling effect and the cavity frequency-dependent modification of the rate constant. Future theoretical works as suggested above are needed to fully resolve these mysteries of vibrational strong coupling modified reactivities inside an optical cavity.

SUPPLEMENTARY MATERIAL

See the supplementary material for the details of the Hessian matrix of the model system, invariance of the barrier height and k_{TST} upon changing light–matter coupling, an approximate expression of $\Omega_-^\ddagger$, cavity dissipation, and numerical simulations.

ACKNOWLEDGMENTS

This work was supported by the National Science Foundation CAREER Award under Grant No. CHE-1845747, a Cottrell Scholar award (a program by Research Corporation for Science Advancement), and a University Research Award from the University of Rochester. Computing resources were provided by the Center for Integrated Research Computing (CIRC) at the University of Rochester. The authors appreciate valuable discussions and comments from Mike Taylor, Eric Koessler, and Braden Weight. The authors also appreciate the help from two reviewers and the journal editor to improve the quality of this paper.

AUTHOR DECLARATIONS

Conflict of Interest

The authors have no conflicts to disclose.

DATA AVAILABILITY

The data that support the findings of this study are available from the corresponding author upon reasonable request.

REFERENCES

[1] J. George, T. Chervy, A. Shalabney, E. Devaux, H. Hiura, C. Genet, and T. W. Ebbesen, "Multiple Rabi splittings under ultra-strong vibrational coupling," Phys. Rev. Lett. **117**, 153601 (2016).

[2] A. Shalabney, J. George, J. Hutchison, G. Pupillo, C. Genet, and T. W. Ebbesen, "Coherent coupling of molecular resonators with a microcavity mode," Nat. Commun. **6**, 5981 (2015).

[3] A. Thomas, L. Lethuillier-Karl, K. Nagarajan, R. M. A. Vergauwe, J. George, T. Chervy, A. Shalabney, E. Devaux, C. Genet, J. Moran, and T. W. Ebbesen, "Tilting a ground-state reactivity landscape by vibrational strong coupling," Science **363**, 615–619 (2019).

[4] A. Thomas, J. George, A. Shalabney, M. Dryzhakov, S. J. Varma, J. Moran, T. Chervy, X. Zhong, E. Devaux, C. Genet, J. A. Hutchison, and T. W. Ebbesen, "Ground-state chemical reactivity under vibrational coupling to the vacuum electromagnetic field," Angew. Chem. **128**, 11634–11638 (2016).

[5] A. Thomas, A. Jayachandran, L. Lethuillier-Karl, R. M. A. Vergauwe, K. Nagarajan, E. Devaux, C. Genet, J. Moran, and T. W. Ebbesen, "Ground state chemistry under vibrational strong coupling: Dependence of thermodynamic parameters on the Rabi splitting energy," Nanophotonics **9**, 249–255 (2020).

[6] R. M. A. Vergauwe, A. Thomas, K. Nagarajan, A. Shalabney, J. George, T. Chervy, M. Seidel, E. Devaux, V. Torbeev, and T. W. Ebbesen, "Modification of enzyme activity by vibrational strong coupling of water," Angew. Chem., Int. Ed. **58**, 15324–15328 (2019).

[7] K. Hirai, R. Takeda, J. A. Hutchison, and H. Uji-i, "Modulation of Prins cyclization by vibrational strong coupling," Angew. Chem., Int. Ed. **59**, 5332–5335 (2020).

[8] J. Lather, P. Bhatt, A. Thomas, T. W. Ebbesen, and J. George, "Cavity catalysis by cooperative vibrational strong coupling of reactant and solvent molecules," Angew. Chem., Int. Ed. **58**, 10635–10638 (2019).

[9] J. Lather, A. N. K. Thabassum, J. Singh, and J. George, "Cavity catalysis: Modifying linear free-energy relationship under cooperative vibrational strong coupling," Chem. Sci. (online 2021).

[10] T. E. Li, A. Nitzan, and J. E. Subotnik, "Collective vibrational strong coupling effects on molecular vibrational relaxation and energy transfer: Numerical insights via cavity molecular dynamics simulations," Angew. Chem. **133**, 15661–15668 (2021).

[11] M. Du and J. Yuen-Zhou, "Can dark states explain vibropolaritonic chemistry?," arXiv:2104.07214 (2021).

[12] X. Li, A. Mandal, and P. Huo, "Cavity frequency-dependent theory for vibrational polariton chemistry," Nat. Commun. **12**, 1315 (2021).

[13] C. Climent and J. Feist, "On the S_N2 reactions modified in vibrational strong coupling experiments: Reaction mechanisms and vibrational mode assignments," Phys. Chem. Chem. Phys. **22**, 23545–23552 (2020).

[14] M. Du, J. A. Campos-Gonzalez-Angulo, and J. Yuen-Zhou, "Nonequilibrium effects of cavity leakage and vibrational dissipation in thermally-activated polariton chemistry," J. Chem. Phys. **154**, 084108 (2021).

[15] T. E. Li, A. Nitzan, and J. E. Subotnik, "On the origin of ground-state vacuum-field catalysis: Equilibrium consideration," J. Chem. Phys. **152**, 234107 (2020).

[16] C. Schafer, J. Flick, E. Ronca, P. Narang, and A. Rubio, "Shining light on the microscopic resonant mechanism responsible for cavity-mediated chemical reactivity," arXiv:2104.12429 (2021).

[17] P.-Y. Yang and J. Cao, "Quantum effects in chemical reactions under polaritonic vibrational strong coupling," J. Phys. Chem. Lett. **12**, 9531–9538 (2021).

[18] D. S. Wang, T. Neuman, S. F. Yelin, and J. Flick, "Cavity-modified unimolecular dissociation reactions via intramolecular vibrational energy redistribution," arXiv:2109.06631 (2021).

[19] J. A. Campos-Gonzalez-Angulo and J. Yuen-Zhou, "Polaritonic normal modes in transition state theory," J. Chem. Phys. **152**, 161101 (2020).

[20] X. Li, A. Mandal, and P. Huo, "Theory of mode-selective chemistry through polaritonic vibrational strong coupling," J. Phys. Chem. Lett. **12**, 6974–6982 (2021).

[21] J. Galego, C. Climent, F. J. Garcia-Vidal, and J. Feist, "Cavity Casimir-Polder forces and their effects in ground-state chemical reactivity," Phys. Rev. X **9**, 021057 (2019).

[22] J. A. Campos-Gonzalez-Angulo, R. F. Ribeiro, and J. Yuen-Zhou, "Resonant catalysis of thermally activated chemical reactions with vibrational polaritons," Nat. Commun. **10**, 4685 (2019).

[23] H. Hiura, A. Shalabney, and J. George, "A reaction kinetic model for vacuum-field catalysis based on vibrational light-matter coupling," chemRxiv:9275777.v1 (2019).

[24] E. A. Power and S. Zienau, "Coulomb gauge in non-relativistic quantum electrodynamics and the shape of spectral lines," Philos. Trans. R. Soc. London, Ser. A **251**, 427–454 (1959).

[25] C. Cohen-Tannoudji, J. Dupont-Roc, and G. Grynberg, *Photons and Atoms: Introduction to Quantum Electrodynamics* (John Wiley & Sons, Inc., Hoboken, 1989).

[26] V. Rokaj, D. M. Welakuh, M. Ruggenthaler, and A. Rubio, "Light–matter interaction in the long-wavelength limit: No ground-state without dipole self-energy," J. Phys. B: At., Mol. Opt. Phys. **51**, 034005 (2018).

[27] C. Schäfer, M. Ruggenthaler, V. Rokaj, and A. Rubio, "Relevance of the quadratic diamagnetic and self-polarization terms in cavity quantum electrodynamics," ACS Photonics **7**, 975–990 (2020).

[28] M. A. D. Taylor, A. Mandal, W. Zhou, and P. Huo, "Resolution of gauge ambiguities in molecular cavity quantum electrodynamics," Phys. Rev. Lett. **125**, 123602 (2020).

[29] D. D. Bernardis, P. Pilar, T. Jaako, S. D. Liberato, and P. Rabl, "Breakdown of gauge invariance in ultrastrong-coupling cavity QED," Phys. Rev. A **98**, 053819 (2018).

[30] M. Lilichenko and D. V. Matyushov, "Control of electron transfer rates in liquid crystalline media," J. Phys. Chem. B **107**, 1937–1940 (2003).

[31] T. Kato, M. Yoshio, T. Ichikawa, B. Soberats, H. Ohno, and M. Funahashi, "Transport of ions and electrons in nanostructured liquid crystals," Nat. Rev. Mater. **2**, 17001 (2017).

[32] P. Kokhanchik, H. Sigurdsson, B. Piętka, J. Szczytko, and P. G. Lagoudakis, "Photonic Berry curvature in double liquid crystal microcavities with broken inversion symmetry," Phys. Rev. B **103**, L081406 (2021).

[33] K. Rechcinska, M. Król, R. Mazur, P. Morawiak, R. Mirek, K. łempicka, W. Bardyszewski, M. Matuszewski, P. Kula, W. Piecek, P. G. Lagoudakis, B. Pietka, and J. Szczytko, "Engineering spin-orbit synthetic Hamiltonians in liquid-crystal optical cavities," Science **366**, 727–730 (2019).

[34] Indeed, if $\hat{\mathcal{I}} = \hat{\mathcal{P}} + \hat{\mathcal{Q}}$ represents the identity of the full electronic Hilbert space, then $\hat{\mathcal{P}}\hat{\mu}\hat{\mathcal{P}}$ is properly confined in the subspace $\hat{\mathcal{P}}$, whereas $\hat{\mathcal{P}}\hat{\mu}^2\hat{\mathcal{P}} = \hat{\mathcal{P}}\hat{\mu}(\hat{\mathcal{P}} + \hat{\mathcal{Q}})\hat{\mu}\hat{\mathcal{P}}$ contains the terms outside the subspace $\hat{\mathcal{P}}$. More numerical evidence can be found in Fig. S2 of the supplementary material in Ref. 28.

[35] A. O. Caldeira and A. J. Leggett, "Influence of dissipation on quantum tunneling in macroscopic systems," Phys. Rev. Lett. **46**, 211–214 (1981).

[36] K. H. Hughes, C. D. Christ, and I. Burghardt, "Effective-mode representation of non-Markovian dynamics: A hierarchical approximation of the spectral density. I. Application to single surface dynamics," J. Chem. Phys. **131**, 024109 (2009).

[37] G. Hanna and R. Kapral, "Quantum-classical Liouville dynamics of nonadiabatic proton transfer," J. Chem. Phys. **122**, 244505 (2005).

[38] T. Yamamoto and W. H. Miller, "Path integral evaluation of the quantum instanton rate constant for proton transfer in a polar solvent," J. Chem. Phys. **122**, 044106 (2005).

[39] R. Collepardo-Guevara, I. R. Craig, and D. E. Manolopoulos, "Proton transfer in a polar solvent from ring polymer reaction rate theory," J. Chem. Phys. **128**, 144502 (2008).

[40] B. J. Ka and W. H. Thompson, "Nonadiabatic effects on proton transfer rate constants in a nanoconfined solvent," J. Phys. Chem. B **114**, 7535–7542 (2010).

[41] I. R. Craig, M. Thoss, and H. Wang, "Accurate quantum-mechanical rate constants for a linear response Azzouz-Borgis proton transfer model employing the multilayer multiconfiguration time-dependent Hartree approach," J. Chem. Phys. **135**, 064504 (2011).

[42] H. Azzouz and D. Borgis, "A quantum molecular-dynamics study of proton-transfer reactions along asymmetrical H bonds in solution," J. Chem. Phys. **98**, 7361–7374 (1993).

[43] S. Hammes-Schiffer and J. C. Tully, "Proton transfer in solution: Molecular dynamics with quantum transitions," J. Chem. Phys. **101**, 4657–4667 (1994).

[44]S. Y. Kim and S. Hammes-Schiffer, "Molecular dynamics with quantum transitions for proton transfer: Quantum treatment of hydrogen and donor–acceptor motions," J. Chem. Phys. **119**, 4389–4398 (2003).
[45]R. P. McRae, G. K. Schenter, B. C. Garrett, Z. Svetlicic, and D. G. Truhlar, "Variational transition state theory evaluation of the rate constant for proton transfer in a polar solvent," J. Chem. Phys. **115**, 8460–8480 (2001).
[46]D. Antoniou and S. D. Schwartz, "A molecular dynamics quantum Kramers study of proton transfer in solution," J. Chem. Phys. **110**, 465–472 (1999).
[47]D. Antoniou and S. D. Schwartz, "Quantum proton transfer with spatially dependent friction: Phenol-amine in methyl chloride," J. Chem. Phys. **110**, 7359–7364 (1999).
[48]L. Chen and Q. Shi, "Quantum rate dynamics for proton transfer reactions in condensed phase: The exact hierarchical equations of motion approach," J. Phys. Chem. **130**, 134505 (2009).
[49]Q. Shi, L. Zhu, and L. Chen, "Quantum rate dynamics for proton transfer reaction in a model system: Effect of the rate promoting vibrational mode," J. Chem. Phys. **135**, 044505 (2011).
[50]W. Xie, Y. Xu, L. Zhu, and Q. Shi, "Mixed quantum classical calculation of proton transfer reaction rates: From deep tunneling to over the barrier regimes," J. Chem. Phys. **140**, 174105 (2014).
[51]J. Flick, H. Appel, M. Ruggenthaler, and A. Rubio, "Cavity Born–Oppenheimer approximation for correlated electron–nuclear-photon systems," J. Chem. Theory Comput. **13**, 1616–1625 (2017).
[52]D. Frenkel and B. Smit, *Understanding Molecular Simulation* (Elsevier, San Diego, 2002).
[53]W. H. Miller, S. D. Schwartz, and J. W. Tromp, "Quantum mechanical rate constants for bimolecular reactions," J. Chem. Phys. **79**, 4889–4898 (1983).
[54]D. Chandler and D. Wu, *Introduction to Modern Statistical Mechanics* (Oxford University Press, Oxford, 1987).
[55]V. P. Zhdanov, "Vacuum field in a cavity, light-mediated vibrational coupling, and chemical reactivity," Chem. Phys. **535**, 110767 (2020).
[56]P. Hänggi, P. Talkner, and M. Borkovec, "Reaction-rate theory: Fifty years after Kramers," Rev. Mod. Phys. **62**, 251–341 (1990).
[57]E. W. Fischer and P. Saalfrank, "Ground state properties and infrared spectra of anharmonic vibrational polaritons of small molecules in cavities," J. Chem. Phys. **154**, 104311 (2021).
[58]R. F. Grote and J. T. Hynes, "The stable states picture of chemical reactions. II. Rate constants for condensed and gas phase reaction models," J. Chem. Phys. **73**, 2715–2732 (1980).
[59]B. J. Gertner, K. R. Wilson, and J. T. Hynes, "Nonequilibrium solvation effects on reaction rates for model S_N2 reactions in water," J. Chem. Phys. **90**, 3537–3558 (1989).
[60]P. Hanggi and F. Mojtabai, "Thermally activated escape rate in presence of long-time memory," Phys. Rev. A **26**, 1168–1170 (1982).
[61]B. Carmeli and A. Nitzan, "Non-Markovian theory of activated rate processes. III. Bridging between the Kramers limits," Phys. Rev. A **29**, 1481–1495 (1984).
[62]S. C. Tucker, M. E. Tuckerman, B. J. Berne, and E. Pollak, "Comparison of rate theories for generalized Langevin dynamics," J. Chem. Phys. **95**, 5809–5826 (1991).
[63]H. Eyring, "The activated complex in chemical reactions," J. Chem. Phys. **3**, 107–115 (1935).
[64]N. B. Slater, "New formulation of gaseous unimolecular dissociation rates," J. Chem. Phys. **24**, 1256–1257 (1956).
[65]E. Pollak, "Theory of activated rate processes: A new derivation of Kramers' expression," J. Chem. Phys. **85**, 865–867 (1986).
[66]I. S. Novikov, Y. V. Suleimanov, and A. V. Shapeev, "Automated calculation of thermal rate coefficients using ring polymer molecular dynamics and machine-learning interatomic potentials with active learning," Phys. Chem. Chem. Phys. **20**, 29503–29512 (2018).
[67]J. Zuo, Y. Li, H. Guo, and D. Xie, "Rate coefficients of the HCl + OH → Cl + H_2O reaction from ring polymer molecular dynamics," J. Phys. Chem. A **120**, 3433–3440 (2016).
[68]B. Peters, *Reaction Rate Theory and Rare Event* (Elsevier, Amsterdam, 2017).
[69]G. van der Zwan and J. T. Hynes, "Dynamical polar solvent effects on solution reactions: A simple continuum model," J. Chem. Phys. **76**, 2993–3001 (1982).
[70]N. E. Henriksen and F. Y. Hansen, *Theories of Molecular Reaction Dynamics: The Microscopic Foundation of Chemical Kinetics* (Oxford University Press, Oxford, 2008).
[71]R. F. Ribeiro, L. A. Martínez-Martínez, M. Du, J. Campos-Gonzalez-Angulo, and J. Yuen-Zhou, "Polariton chemistry: Controlling molecular dynamics with optical cavities," Chem. Sci. **9**, 6325–6339 (2018).
[72]L. Qiu, A. Mandal, O. Morshed, M. T. Meidenbauer, W. Girten, P. Huo, A. N. Vamivakas, and T. D. Krauss, "Molecular polaritons generated from strong coupling between CDSE nanoplatelets and a dielectric optical cavity," J. Phys. Chem. Lett. **12**, 5030–5038 (2021).
[73]D. M. Coles, P. Michetti, C. Clark, W. C. Tsoi, A. M. Adawi, J.-S. Kim, and D. G. Lidzey, "Vibrationally assisted polariton-relaxation processes in strongly coupled organic-semiconductor microcavities," Adv. Funct. Mater. **21**, 3691–3696 (2011).
[74]J. del Pino, F. A. Y. N. Schröder, A. W. Chin, J. Feist, and F. J. Garcia-Vidal, "Tensor network simulation of non-Markovian dynamics in organic polaritons," Phys. Rev. Lett. **121**, 227401 (2018).
[75]J. Lather and J. George, "Improving enzyme catalytic efficiency by co-operative vibrational strong coupling of water," J. Phys. Chem. Lett. **12**, 379–384 (2021).
[76]H. Hiura and A. Shalabney, "Vacuum-field catalysis: Accelerated reactions by vibrational ultra strong coupling," chemRxiv:7234721.v5 (2019).
[77]M. V. Imperatore, J. B. Asbury, and N. C. Giebink, "Reproducibility of cavity-enhanced chemical reaction rates in the vibrational strong coupling regime," J. Chem. Phys. **154**, 191103 (2021).